Title
Synergistic chemotherapy by combined moderate hyperthermia and photochemical internalization.

Journal
Biomedical Optics Express, 7(4)

ISSN
2156-7085

Authors
Christie, Catherine
Molina, Stephanie
Gonzales, Jonathan
et al.

Publication Date
2016-04-01

DOI
10.1364/boe.7.001240

Peer reviewed

Biomedical Optics EXPRESS

Synergistic chemotherapy by combined moderate hyperthermia and photochemical internalization

Catherine Christie,[1,*] Stephanie Molina,[2] Jonathan Gonzales,[1] Kristian Berg,[3] Rohit Kumar Nair,[1] Khoi Huynh,[1] Steen J. Madsen,[2] and Henry Hirschberg[1,2]

[1]*Beckman Laser Institute, University of California, Irvine,, Irvine, CA 92612 USA*
[2]*Department of Health Physics and Diagnostic Sciences, University of Nevada, Las Vegas, NV 89154, USA*
[3]*Dept. of Radiation Biology The Norwegian Radium Hospital, Oslo University Hospital, Oslo Norway*
[*]*cchrist1@uci.edu*

Abstract: Combination therapies of photochemical internalization (PCI) and moderate hyperthermia (MHT) were investigated in an *in vitro* system consisting of human and rat glioma spheroids. PCI using the amphiphilic photosensitizer, AlPcS2a and two anti cancer agents BLM or 5-FU were used. Spheroids were irradiated with λ = 670 nm laser light in an incubator at temperatures ranging from 37 to 44°C. For each temperature investigated, spheroids were divided into 4 groups: control, drug-only, photodynamic therapy (PDT), and PCI. PDT and PCI spheroids were exposed to radiant exposures ranging from 0.3 to 2.5 J cm^{-2} using an irradiance of 5 mW cm^{-2}. Toxicity was evaluated from spheroid growth kinetics. The combination of PCI and MHT resulted in significant increases in BLM efficacy at 44°C for both cell line derived spheroids compared to controls at 37°C over the range of radiant exposures examined. 5-FU PCI was ineffective for the human cell line at both 37 and 44°C.

OCIS codes: (140.0140) Lasers and laser optics; (140.3070) Infrared and far-infrared lasers.

References and links

1. M. C. Chamberlain, "Radiographic patterns of relapse in glioblastoma," J. Neurooncol. **101**(2), 319–323 (2011).
2. M. C. Dobelbower, O. L. Burnett III, R. A. Nordal, L. B. Nabors, J. M. Markert, M. D. Hyatt, and J. B. Fiveash, "Patterns of failure for glioblastoma multiforme following concurrent radiation and temozolomide," J. Med. Imaging Radiat. Oncol. **55**(1), 77–81 (2011).
3. R. Stupp, M. E. Hegi, W. P. Mason, M. J. van den Bent, M. J. Taphoorn, R. C. Janzer, S. K. Ludwin, A. Allgeier, B. Fisher, K. Belanger, P. Hau, A. A. Brandes, J. Gijtenbeek, C. Marosi, C. J. Vecht, K. Mokhtari, P. Wesseling, S. Villa, E. Eisenhauer, T. Gorlia, M. Weller, D. Lacombe, J. G. Cairncross, and R. O. Mirimanoff; European Organisation for Research and Treatment of Cancer Brain Tumour and Radiation Oncology Groups; National Cancer Institute of Canada Clinical Trials Group, "Effects of radiotherapy with concomitant and adjuvant temozolomide versus radiotherapy alone on survival in glioblastoma in a randomised phase III study: 5-year analysis of the EORTC-NCIC trial," Lancet Oncol. **10**(5), 459–466 (2009).
4. S. B. Field and N. M. Bleehen, "Hyperthermia in the treatment of cancer," Cancer Treat. Rev. **6**(2), 63–94 (1979).
5. R. Valdagni, F. F. Liu, and D. S. Kapp, "Important prognostic factors influencing outcome of combined radiation and hyperthermia," Int. J. Radiat. Oncol. Biol. Phys. **15**(4), 959–972 (1988).
6. P. Wust, B. Hildebrandt, G. Sreenivasa, B. Rau, J. Gellermann, H. Riess, R. Felix, and P. M. Schlag, "Hyperthermia in Combined Treatment of Cancer," Lancet Oncol. **3**(8), 487–497 (2002).
7. J. van der Zee, "Heating the patient: A promising approach?" Ann. Oncol. **13**(8), 1173–1184 (2002).
8. N. G. Huilgol, S. Gupta, and R. Dixit, "Chemoradiation with hyperthermia in the treatment of head and neck cancer," Int. J. Hyperthermia **26**(1), 21–25 (2010).
9. G. M. Hahn, J. Braun, and I. Har-Kedar, "Thermochemotherapy: synergism between hyperthermia (42-43 degrees) and adriamycin (of bleomycin) in mammalian cell inactivation," Proc. Natl. Acad. Sci. U.S.A. **72**(3), 937–940 (1975).
10. H. H. Kampinga and E. Dikomey, "Hyperthermic radiosensitization: mode of action and clinical relevance," Int. J. Radiat. Biol. **77**(4), 399–408 (2001).

#255220 Received 6 Jan 2016; revised 4 Feb 2016; accepted 10 Feb 2016; published 14 Mar 2016

11. J. Michalakis, S. D. Georgatos, E. de Bree, H. Polioudaki, J. Romanos, V. Georgoulias, D. D. Tsiftsis, and P. A. Theodoropoulos, "Short-term exposure of cancer cells to micromolar doses of paclitaxel, with or without hyperthermia, induces long-term inhibition of cell proliferation and cell death in vitro," Ann. Surg. Oncol. **14**(3), 1220–1228 (2007).
12. M. O. Dereski, L. Madigan, and M. Chopp, "The effect of hypothermia and hyperthermia on photodynamic therapy of normal brain," Neurosurgery **36**(1), 141–146 (1995).
13. Q. Chen, H. Chen, H. Shapiro, and F. W. Hetzel, "Sequencing of combined hyperthermia and photodynamic therapy," Radiat. Res. **146**(3), 293–297 (1996).
14. H. Hirschberg, C. H. Sun, B. J. Tromberg, A. T. Yeh, and S. J. Madsen, "Enhanced cytotoxic effects of 5-aminolevulinic acid-mediated photodynamic therapy by concurrent hyperthermia in glioma spheroids," J. Neurooncol. **70**(3), 289–299 (2004).
15. K. Berg, M. Folini, L. Prasmickaite, P. K. Selbo, A. Bonsted, B. Ø. Engesæter, N. Zaffaroni, A. Weyergang, A. Dietze, G. M. Maelandsmo, E. Wagner, O. J. Norum, and A. Høgset, "Photochemical internalization: a new tool for drug delivery," Curr. Pharm. Biotechnol. **8**(6), 362–372 (2007).
16. P. K. Selbo, A. Weyergang, A. Høgset, O. J. Norum, M. B. Berstad, M. Vikdal, and K. Berg, "Photochemical internalization provides time- and space-controlled endolysosomal escape of therapeutic molecules," J. Control. Release **148**(1), 2–12 (2010).
17. M. S. Mathews, J. W. Blickenstaff, E. C. Shih, G. Zamora, V. Vo, C. H. Sun, H. Hirschberg, and S. J. Madsen, "Photochemical internalization of bleomycin for glioma treatment," J. Biomed. Opt. **17**(5), 058001 (2012).
18. A. Weyergang, M. E. Berstad, B. Bull-Hansen, C. E. Olsen, P. K. Selbo, and K. Berg, "Photochemical activation of drugs for the treatment of therapy-resistant cancers," Photochem. Photobiol. Sci. **14**(8), 1465–1475 (2015).
19. H. Kim, D. Lee, J. Kim, T. I. Kim, and W. J. Kim, "Photothermally triggered cytosolic drug delivery via endosome disruption using a functionalized reduced graphene oxide," ACS Nano **7**(8), 6735–6746 (2013).
20. D. Ma, "Enhancing endosomal escape for nanoparticle mediated siRNA delivery," Nanoscale **6**(12), 6415–6425 (2014).
21. B. Drewinko, T. L. Loo, B. Brown, J. A. Gottlieb, and E. J. Freireich, "Combination chemotherapy in vitro with adriamycin. Observations of additive, antagonistic, and synergistic effects when used in two-drug combinations on cultured human lymphoma cells," Cancer Biochem. Biophys. **1**(4), 187–195 (1976).
22. M. A. Mackey and J. L. Roti Roti, "A model of heat-induced clonogenic cell death," J. Theor. Biol. **156**(2), 133–146 (1992).
23. B. Hildebrandt, P. Wust, O. Ahlers, A. Dieing, G. Sreenivasa, T. Kerner, R. Felix, and H. Riess, "The cellular and molecular basis of hyperthermia," Crit. Rev. Oncol. Hematol. **43**(1), 33–56 (2002).
24. J. Zhou, X. Wang, L. Du, L. Zhao, F. Lei, W. Ouyang, Y. Zhang, Y. Liao, and J. Tang, "Effect of hyperthermia on the apoptosis and proliferation of CaSki cells," Mol. Med. Rep. **4**(1), 187–191 (2011).
25. O. Dahl, "Mechanism of thermal enhancement of chemotherapeutic cytotoxicity," Hyperthermia and Oncology. Utrecht: VSP, 29 (1994).
26. R. Issels, "Hyperthermia combined with chemotherapy-biological rationale, clinical application, and treatment results," Onkologie **22**(5), 374–381 (1999).
27. R. F. Barth, "Rat brain tumor models in experimental neuro-oncology: the 9L, C6, T9, F98, RG2 (D74), RT-2 and CNS-1 gliomas," J. Neurooncol. **36**(1), 91–102 (1998).
28. S. M. Hecht, "DNA strand scission by activated bleomycin group antibiotics," Fed. Proc. **45**(12), 2784–2791 (1986).
29. C. Tysoe and S. G. Withers, "Fluorinated mechanism-based inhibitors: common themes and recent developments," Curr. Top. Med. Chem. **14**(7), 865–874 (2014).
30. L. R. Hirsch, R. J. Stafford, J. A. Bankson, S. R. Sershen, B. Rivera, R. E. Price, J. D. Hazle, N. J. Halas, and J. L. West, "Nanoshell-mediated near-infrared thermal therapy of tumors under magnetic resonance guidance," Proc. Natl. Acad. Sci. U.S.A. **100**(23), 13549–13554 (2003).
31. X. Huang, P. K. Jain, I. H. El-Sayed, and M. A. El-Sayed, "Determination of the minimum temperature required for selective photothermal destruction of cancer cells with the use of immunotargeted gold nanoparticles," Photochem. Photobiol. **82**(2), 412–417 (2006).
32. J. A. Schwartz, A. M. Shetty, R. E. Price, R. J. Stafford, J. C. Wang, R. K. Uthamanthil, K. Pham, R. J. McNichols, C. L. Coleman, and J. D. Payne, "Feasibility study of particle-assisted laser ablation of brain tumors in orthotopic canine model," Cancer Res. **69**(4), 1659–1667 (2009).
33. C. Christie, S. J. Madsen, Q. Peng, and H. Hirschberg, "Macrophages as nanoparticle delivery vectors for photothermal therapy of brain tumors," Ther. Deliv. **6**(3), 371–384 (2015).
34. A. J. Trinidad, S. J. Hong, Q. Peng, S. J. Madsen, and H. Hirschberg, "Combined concurrent photodynamic and gold nanoshell loaded macrophage-mediated photothermal therapies: an in vitro study on squamous cell head and neck carcinoma," Lasers Surg. Med. **46**(4), 310–318 (2014).
35. Y. Tang and A. J. McGoron, "Combined effects of laser-ICG photothermotherapy and doxorubicin chemotherapy on ovarian cancer cells," J. Photochem. Photobiol. B **97**(3), 138–144 (2009).
36. J. G. Mehtala, S. Torregrosa-Allen, B. D. Elzey, M. Jeon, C. Kim, and A. Wei, "Synergistic effects of cisplatin chemotherapy and gold nanorod-mediated hyperthermia on ovarian cancer cells and tumors," Nanomedicine (Lond.) **9**(13), 1939–1955 (2014).

#255220 Received 6 Jan 2016; revised 4 Feb 2016; accepted 10 Feb 2016; published 14 Mar 2016

1. Introduction

Despite employing improved surgical techniques and imaging modalities now available followed by radiation and chemotherapy, the great majority of glioma patients do suffer a recurrence of their tumors. Greater than 80% of tumor recurrences occur around the margins of the surgical resection cavity [1, 2]. Although chemotherapy has proven effective for the treatment of many tumor types, survival benefits in malignant glioma patients have been modest [3]. In order to improve the effects of conventional therapies, moderate hyperthermia (MHT) has been combined with chemotherapy or ionizing radiation in the treatment of a variety of tumors as adjuvant therapy [4–8]. MHT typically occurs in a temperature range of 40 to 44°C over times ranging from 30–60 min and is generally nontoxic to cells [7]. Nevertheless MHT has been shown to increase the efficacy of a number of cytotoxic drugs [9–11].

Photophrin based photodynamic therapy (PDT) has also been used in combination with MHT both *in vivo* and *in vitro*. For example, Dereski et al. [12] found that the effects were greater than additive when MHT was given post-PDT. Using a murine mammary adenocarcinoma model, Chen et al. [13] showed that the combination of PDT and MHT produced a synergetic tumor response. Hirschberg et al. [14] examined synergistic effects of 5-aminolevulinic acid-mediated PDT and MHT concurrently on human and rat glioma spheroids. These latter results showed that, when administered separately, PDT and HT at suboptimal levels were not very effective, however, concurrent administration of the two treatment modalities at these same levels resulted in significant spheroid growth inhibition.

PCI, based on the principles of PDT, is a technique that improves the utilization of macromolecules in cancer therapy in a site-specific manner [15–18]. The concept is based on the use of specially designed photosensitizers, with two sulfonate groups on adjacent phenyl rings such as TPPS2a AlPcS2a and TPCS2a, that localize preferentially in the membranes of endocytic vesicles. Upon exposure to light of appropriate wavelengths (usually in the far red of the visible spectrum), the photosensitizers induce the formation of reactive oxygen species, in particular, singlet molecular oxygen. The photo-oxidation of the endocytic membranes leads to the release of the contents of these vesicles into the cytosol. In this way, macromolecules encapsulated in the endosome will reach the cytosol and exert their biological activity instead of being degraded by lysosomal hydrolases. MHT has also been shown to induce endosomal escape [19, 20]. It was therefore of interest to examine if the effects of MHT in combination with PCI would enhance drug efficacy in a synergistic manner. Combinational therapies were examined in an *in vitro* system consisting of human and rat glioma spheroids. As opposed to cell monolayers tumor spheroids mimic *in vivo* tumors in their micro-environment in terms of gene expression, oxygen gradient characteristic and the biological behavior of the cells and are well suited to this type of *in vitro* study. Radiant exposures and temperatures were varied in order to evaluate optimum light-temperature combinations as determined from spheroid growth kinetics. The basic concept of MHT enhanced PCI is shown in cartoon form in Fig. 1.

#255220 Received 6 Jan 2016; revised 4 Feb 2016; accepted 10 Feb 2016; published 14 Mar 2016

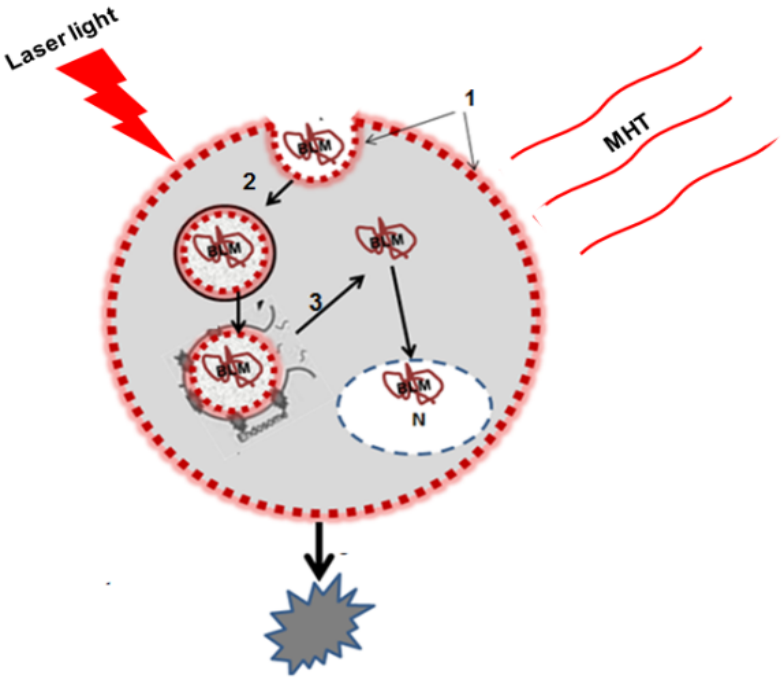

Fig. 1. Endosomal escape of hydrophilic drug by combined MHT and PCI **1.** An amphiphilic photosensitizer is given before administration of the drug. The photosensitizer binds to the plasma membrane and is **2.** taken into the cell together with the drug by endocytosis. The photosensitizer and the drug co-localize in the endosomes. Since the photosensitizer is partly hydrophilic and partly hydrophobic it will remain in the membrane of the endosome, while the hydrophilic drug will localize in the lumen. **3.** Combined thermal and light exposure leads to induced rupture of the endosome with subsequent release of the sequestered drug into the cytosol or nucleus resulting in cell death.

2. Methods

2.1 Cells

The human grade IV glioma cell line (ACBT) developed by G. Granger, University of California, Irvine and the rat glioma line F98 was obtained from the American Type Culture Collection (Manassas, VA, USA) were maintained in Dulbecco's Modified Eagle Medium (DMEM) with high glucose (Life Technologies Corp., Carlsbad, CA, USA) supplemented with 10% fetal bovine serum (FBS), 25 mM HEPES buffer (pH 7.4), penicillin (100 U ml-1) and streptomycin (100 µg ml-1) at 37°C and 5% CO_2.

2.2 Spheroid formation

Spheroid generation: MGS were formed by a modification of the centrifugation method as previously described [17]. Briefly, 2.5×10^3 cells in 200 µl of culture medium per well were alloquated into the wells of ultra-low attachment surface 96-well round-bottomed plates (Corning In., NY). The plates were centrifuged at 1000g for 30 minutes. Immediately following centrifugation the tumor cells formed into a disk shape. The plates were maintained at 37°C in a 5% CO_2 incubator for 24 h to allow them to take on the usual 3-dimensional spheroid form.

2.3 Moderate hyperthermia

Drug toxicity. The direct effect of MHT on drug toxicity was examined on spheroids derived from both F98 and ACBT cell lines in the wells of 96 well plates. Forty-eight hours after

#255220 Received 6 Jan 2016; revised 4 Feb 2016; accepted 10 Feb 2016; published 14 Mar 2016

spheroid generation drugs at increasing doses for BLM and 5-FU were added to the wells and the plates were incubated at temperatures of either 37 or 44°C for 45 minutes. The plates were incubated without further wash, at 37°C and were monitored for their growth for an additional 14 days.

PDT and PCI treatments. Twenty four hours after spheroid formation 0.5 μg/mL photosensitizer ($AlPcS_{2a}$; Frontier Scientific Inc., Logan, UT) was added to the wells for an additional 18 h at 37 °C and 5% CO_2. Following incubation, spheroids were washed in the plates and placed into fresh medium in the absence of drug to act as PDT controls. For PCI, the spheroids were incubated in the presence of drug for an additional 4 hours. Following this, the plates were incubated at temperatures of 37, 40 or 44°C for 45 minutes. Light treatment at various radiant exposures at an irradiance of 5 mW/cm^2 was administered with $\lambda = 670$ nm light from a diode laser (Intense; New Jersey USA). Typically, 8-16 spheroids for the various groups were followed in 3 individual trials for up to 14 days of incubation. Culture medium in the wells was exchanged every third day. Determination of spheroid size was carried out by measurement of their diameter using a microscope with a calibrated eyepiece micrometer and their volume calculated assuming a perfect sphere.

Live/dead assay. Forty-eight hours after light treatment, 2-3 spheroids were transferred to glass bottomed imaging dishes, stained using a combination of Hoechst 33342 and Ethidium Homodimer 1 (Life Technologies H1399, Carlsbad, CA) for 1 h, washed and visualized using a two photon inverted Zeiss laser-scanning fluorescent microscope (LSM 410, Carl Zeiss, Jena, Germany). This system allows the differential visualization of cell nuclei using confocal and two-photon microscopy. Simultaneously detected blue and red emissions were isolated by using BP 390-465 IR and BP 565-615 IR band pass filters, respectively. Fluorescent images were pseudo-colored blue (live) and red (dead).

Statistical analysis. All data was analyzed and graphed using Microsoft Excel. The arithmetic mean and standard error were used throughout to calculate averages and errors. Statistical significance was calculated using the Student's t-test as well as the Welch's t-test. Two values were considered distinct when their p-values were below 0.05. In order to determine the degree of interaction between MHT the chemo-agents and PCI the following equation was used [21].

$$\alpha = \frac{SF^{MHT} \, x \, SF^{Chemo}}{SF^{MHT+PCI}} \tag{1}$$

The numerator includes the product of the surviving fraction (SF) of the individual treatments separately and the denominator includes the surviving fraction of the combined treatments. A value of $\alpha = 1$ indicates an additive effect. A value of $\alpha < 1$ or $\alpha > 1$ indicates an antagonistic or synergistic effect, respectively.

3. Results and discussion

3.1 Toxic effects of HT

A temperature of 46°C for 45 min. resulted in total spheroid death for both cell types, while the majority of spheroids subjected to 44°C for the same interval, survived (Fig. 2). Therefore, the hyperthermic threshold was estimated to be between 44 and 46°C. This provided the rationale for the temperature range investigated (37-44°C).

Hyperthermia affects fluidity and stability of cellular membranes and impedes the function of transmembrane transport proteins and cell surface receptors *in vitro*. Additionally, the effects of temperature over 46°C at the cellular level have been shown to inhibit both protein and DNA synthesis. Inhibition of DNA repair enzymes has also been observed as has damage to the cell membrane [22–24]. An increase in temperature leads to higher metabolism which increases the amount of reactive oxygen species (ROS) and damages DNA, proteins, and lipids. In addition to oxidative stress, thermal stress responses include the expression of

#255220 Received 6 Jan 2016; revised 4 Feb 2016; accepted 10 Feb 2016; published 14 Mar 2016

heat shock proteins (HSPs). There is evidence that oxidative stress levels are potentially damaging to proteins, and the up-regulation of HSPs is required to restore the native structures of these damaged proteins.

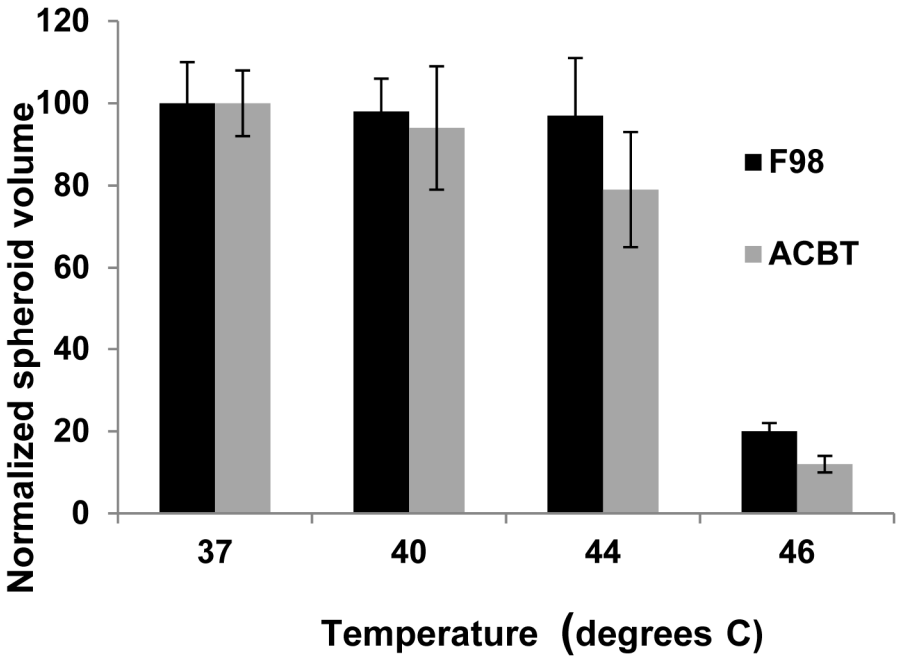

Fig. 2. Effects of temperature on F98 or ACBT spheroid growth: Spheroids, 48 hours after initiation were incubated at temperatures ranging from 37 to 46°C, for 45 minutes. Each data point represents spheroid volume after 2 weeks in culture as a % of 37°C controls and is the mean of 3 experiments. Error bars denote standard errors.

3.2 The effect of MHT on drug toxicity

MHT (41-44°C), while non toxic to cancer cells in and of itself, has been demonstrated to increase the efficacy of chemotherapy in both *in vitro* and *in vivo* experiments [23, 25, 26]. The effects on either F98 or ACBT spheroid growth, of the drugs BLM and 5-FU at 37°C and 44°C were compared. The drug concentrations were varied from 0.0625 to 2.5 and 0.0625-0.025 ug/ml for BLM and 5-FU respectively.

As seen from Fig. 3(a) and 3(b), F98 spheroid growth inhibition was significantly increased at 44°C compared to that seen at 37°C over the 5-FU concentrations tested. In contrast, BLM efficacy was not significantly altered at the two temperatures. Similar results for BLM were obtained for ACBT spheroids (Fig. 3(c)) spheroid growth was inhibited by the drug but displayed little temperature dependence. In contrast, the ACBT cells, derived from a brain tumor patient, were resistant to 5-FU even at high drug concentrations, at both 37 and 44°C (Fig. 3(d)).

#255220 Received 6 Jan 2016; revised 4 Feb 2016; accepted 10 Feb 2016; published 14 Mar 2016

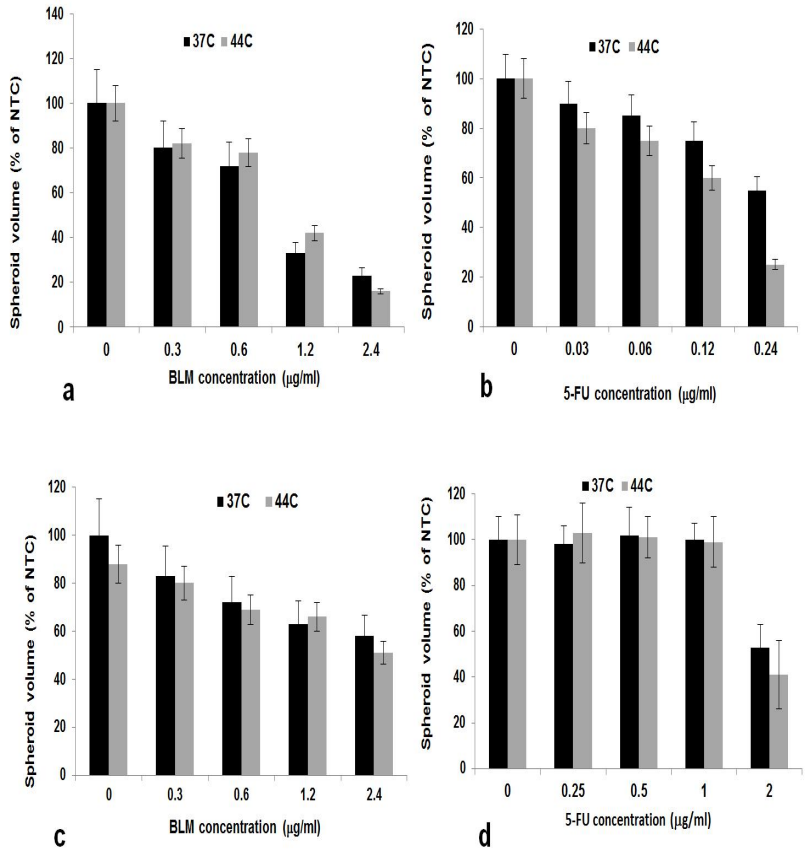

Fig. 3. Effects of MHT on drug toxicity: Spheroids, 48 hours after initiation, were incubated with increasing concentrations of BLM (a, c) or 5-FU (b, d,) at temperatures of 37 or 44°C, for 45 minutes. Incubation was continued at 37°C for an additional 14 days. Each data point represents spheroid volume after 2 weeks in post treatment culture as a % of 37°C controls and is the mean of 3 experiments. Error bars denote standard errors.

3.3 Combined PCI mediated chemotherapy and external induced MHT

In order to investigate the degree of interaction between MHT and PCI suboptimal levels of both drug concentrations and PDT levels, as determined in the above experiments, were used. The effects on drug efficacy of combined concurrent PCI and MHT for both drugs and cell lines are shown in Fig. 4. The drug concentrations used were 0.6 and 0.12 µg/ml for BLM and 5-FU respectively. Sub lethal PDT fluence levels of 0.3 J/cm^2 or 1.5 J/cm^2 resulting in greater than 80% survival were used for F98 or ACBT respectively.

#255220 Received 6 Jan 2016; revised 4 Feb 2016; accepted 10 Feb 2016; published 14 Mar 2016

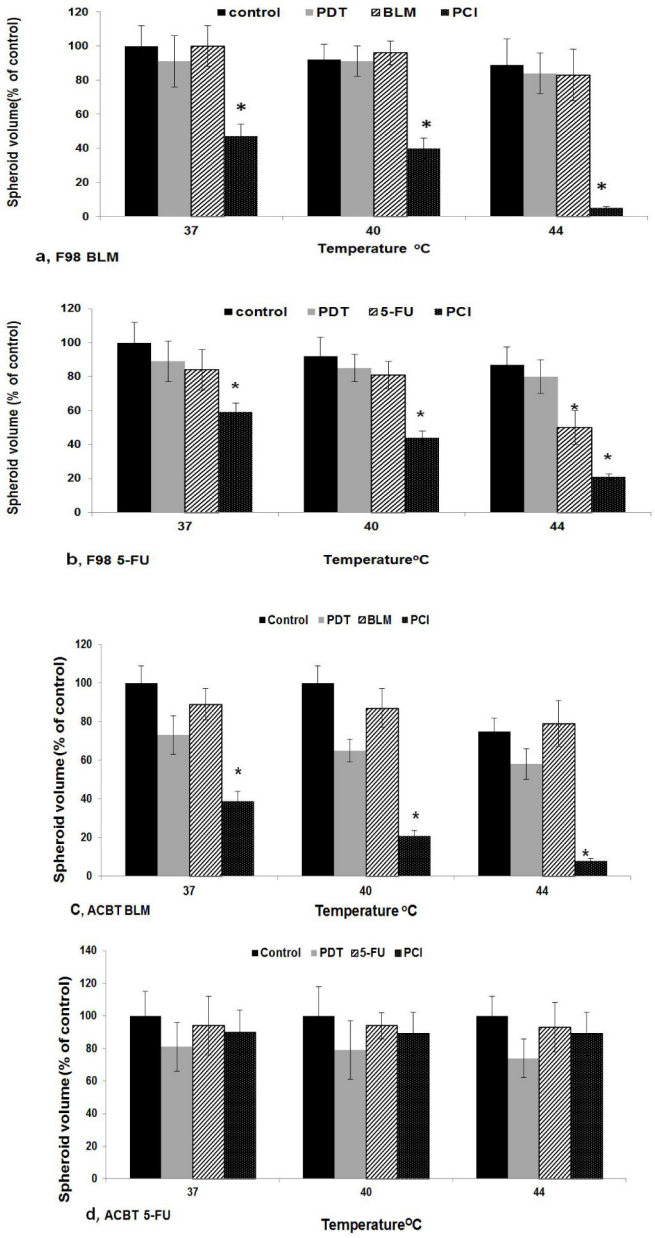

Fig. 4. Effects of MHT on PDT, drug, or PCI on spheroid growth 24 hours after initiation, spheroids undergoing PDT or PCI were incubated with1 μg/ml $AlPcS_{2a}$ for 18 h. Drug concentrations used were 0.6 and 0.12 μg/ml for BLM (Fig. 4 a, c) and 5-FU (Fig. 4 (b, c) respectively. Four hours following drug addition PDT/PCI light treatment at fluence levels of 0.3 J/cm^2 or 1.5 J/cm^2 (F98 Fig. 4 a, b) or (ACBT Fig. 4 c, d). Light treatment was done at 37, 40 or 44°C following a 45 min MHT incubation. Incubation was continued at 37°C for an additional 14 days. Each data point represents spheroid volume after 2 weeks in post treatment culture as a % of 37°C controls at 14 days and is the mean of 3 experiments. Error bars denote standard errors. Asterisks (*) denote significant differences ($p<0.05$) compared to control values.

Spheroid relative growth compared to controls, following 14 days of post treatment incubation, was compared at 37, 40 or 44°C MHT. Student's t-tests were used to verify

#255220 Received 6 Jan 2016; revised 4 Feb 2016; accepted 10 Feb 2016; published 14 Mar 2016

significant differences ($p < 0.05$) between these values and are indicated in Fig. 4 by an asterisk (*). As seen in the figure there was a significant decrease in spheroid growth for both drugs and cell lines at 44°C compared to 37°C ($p < 0.05$).

The degree of synergism for MHT and PCI, as determined by the corresponding α values calculated from Eq (1), are shown in Table 1. As shown in the table, interactions between PCI and MHT at both, 40 and 44°C is synergistic for F98 cell lines for both drugs but only for BLM for the ACBT cell lines.

Table 1. Calculated alpha values for MHT and PCI combination therapies

Temperature	BLM (F98)	5-FU (F98)	BLM (ACBT)	5-FU (ACBT)
44°C	10.1	1.7	5.1	0.79
40°C	2.37	1.36	2.52	0.87
37°C	1.9	1.27	1.69	0.82

In particular, α values for BLM in both cell lines were high (10.1 and 5.1 for F98 and ACBT respectively).

The discrepancy between the effects of MHT and drug or PCI, between F98 and ACBT spheroids, shown in Figs. 3 and 4 might be caused by the differing derivation of the two cell lines used or the different actions of the drugs. The F98 tumor cells are an anaplastic glioma originally derived from transformed fetal CD Fischer rat brain cells following exposure to ethyl-nitrosourea on the twentieth day of gestation [27]. The ACBT line was derived from a patient with a glioblastoma multiforme. 5-FU acts principally as a thymidylate synthase (TS) inhibitor preventing DNA replication, while Bleomycin acts by induction of DNA strand breaks [28, 29].

The kinetics of F98 spheroid growth, following BLM and 5-FU PCI + MHT, were monitored at 1 and 2 weeks post treatment. The drug concentrations used were 0.6 and 0.12 ug/ml for BLM and 5-FU respectively. Sub optimal PDT fluence levels of 0.3 J/cm^2, resulting in greater than 80% survival, were used. Spheroid volume was normalized as a % of non treated 37°C control culture volume on day 14. As seen in Fig. 5 compared to controls, a PCI induced growth delay for PCI was seen for both drugs at 37°C with the spheroids recovering from treatment. In contrast, PCI + MHT at 44°C significantly reduced (for 5-FU) or completely inhibited (for BLM) growth potential.

#255220 Received 6 Jan 2016; revised 4 Feb 2016; accepted 10 Feb 2016; published 14 Mar 2016

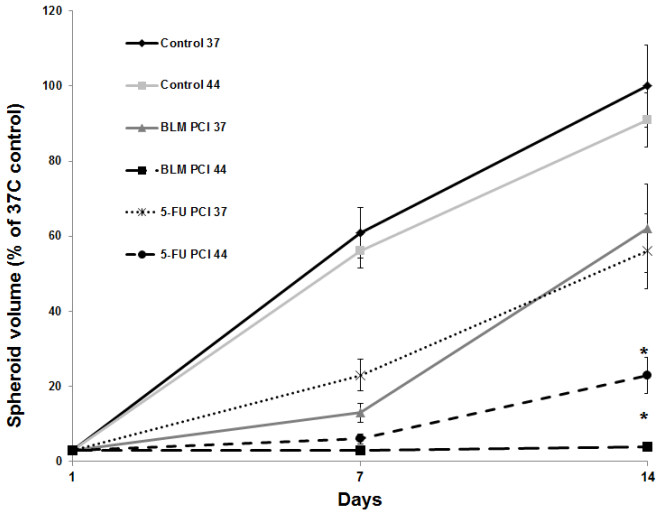

Fig. 5. Kinetics of F98 spheroid growth following MHT-PCI 24 hours after initiation spheroids undergoing PCI were incubated with1 μg/ml $AlPcS_{2a}$ for 18 h. Drug concentrations used were 0.6 and 0.12 ug/ml for BLM and 5-FU respectively. Four hours following drug addition, PCI light treatment at fluence levels of 0.3 J/cm^2 was done at 37 or 44°C following a 45 min MHT incubation. The spheroid volume was evaluated 7 and 14 days post treatment. Each data point represents spheroid volume as a % of 37°C controls at day 14 and is the mean of 3 experiments. Error bars denote standard errors. Asterisks (*) denote significant differences ($p<0.05$) compared to MHT-PCI values at 37°C.

The results of live/dead assay employing two-photon fluorescence images are shown in Fig. 6. As illustrated in Fig. 6(a), virtually no dead cells were observed in control spheroids.

In contrast significantly enhanced toxicity throughout PCI-treated spheroids at 44°C (Fig. 6(c)) compared to that obtained at 37°C (Fig. 5(b)) could be demonstrated. This was inferred from the high proportion of red fluorescing cells observed from the MHT/PCI-treated spheroids (Fig. 6(c)).

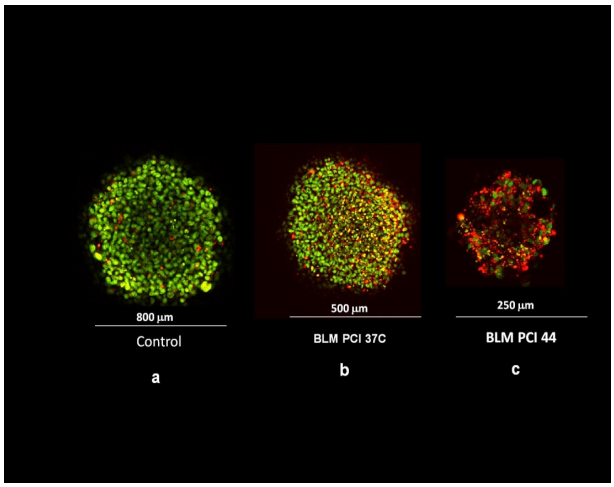

Fig. 6. Live/dead assay of control and or PCI treated spheroids Two-photon fluorescence microscopy images of F98 spheroids stained with Hoechst 33342 (green: live) and Ethidium Homodimer (red: dead). Spheroids were stained 24 h after treatment: **(a)** Control, **(b)** BLM-PCI; 37°C. **(c)** BLM-PCI; 44°C. The images have been cropped, scale bars as shown.

#255220 Received 6 Jan 2016; revised 4 Feb 2016; accepted 10 Feb 2016; published 14 Mar 2016

The mechanism of synergism between MHT and PCI has, at present, not been investigated in detail, but it likely has several components. For efficient drug delivery to take place several extra and intracellular barriers need to be overcome. MHT alone most probably facilitates enhanced drug efficacy by increasing cellular uptake via endocytosis. Both PCI and MHT have been shown to promote endosomal escape and the release of drug into the cytosol [16,19]. In addition, both drugs used in this study are incorporated into DNA causing damage which often results in cell death unless the damage is repaired. Since hyperthermia inhibits DNA repair, it's postulated that the addition of heat enhances the cytotoxicity of the chemotherapeutic agents via inhibition of DNA repair.

In the experiments reported here, MHT was induced externally by exposing the spheroids to elevated temperatures prior to and during PCI treatment. Although this is a convenient method for *in vitro* studies it is not easily adapted to the *in vivo* environment in either experimental animals or patient protocols. An alternative and more selective method for inducing MHT is photothermal therapy (PTT). In one form of PTT electromagnetic radiation (usually in the near-infrared wavelengths) incident on gold-based nanoparticles is converted to heat [30–33]. PTT is an effective method of achieving rapid elevated temperatures in targeted regions in the presence of NIR absorbing gold nanoparticles while limiting damage to normal structures. The efficacy of PTT induced moderate hyperthermia in several forms of combined therapy has been shown to be effective [34–36]. Experiments examining the effects of combined PTT + PCI treatment modalities are in progress.

4. Conclusion

The results of the present study show that MHT and PCI interact in a synergistic manner over a range of light and temperature exposures. The degree of interaction between the two modalities was dependent on both drug type and cell line. The highest degree of interaction was observed for BLM in F98 spheroids and to a lesser extent for the human spheroids. In comparison, the drug 5-FU resulted in only a mild degree of synergism for F98 spheroids while the results in the ACBT spheroids for this drug were antagonistic.

Acknowledgments

The authors are grateful for the support from the Norwegian Radium Hospital Research Foundation. Portions of this work were made possible through access to the LAMMP Program NIBIB P41EB015890 at UCI. Steen Madsen was supported, in part, by the Tony and Renee Marlon Charitable Foundation.

#255220 Received 6 Jan 2016; revised 4 Feb 2016; accepted 10 Feb 2016; published 14 Mar 2016